Synthesis and electrochemical studies of an anthraquinone-conjugated nucleoside and derived oligonucleotides†

Mikkel F. Jacobsen, Elena E. Ferapontova and Kurt V. Gothelf*

Received 25th September 2008, Accepted 18th November 2008
First published as an Advance Article on the web 23rd January 2009
DOI: 10.1039/b816820b

The synthesis of a 2′-deoxyuridine nucleoside linked to an anthraquinone moiety, and its incorporation into oligonucleotides are described, including a facile oxidative demethylation with phenyliodine(III) bis(trifluoroacetate) to reveal the anthraquinone motif. Furthermore, some useful physical and electrochemical properties of the obtained oligonucleotide are also reported, which allow its principal use in electrochemical DNA assays.

Anthraquinone-modified oligonucleotides have proven to be versatile tools in stabilization of duplex DNA by intercalation,[1] electrochemical detection of single-base mismatches (SNPs),[2] and as photoexcitable probes for the study of DNA hole transport.[3] Charge-transfer phenomena in DNA either through oxidative or reductive pathways have received considerable attention in recent years due to their importance in biological environments such protein–DNA complexes, DNA damage, mutations and cancer.[4] As previously employed for pyrene-[5] and phenothiazine-linked nucleosides,[6] we aimed for the synthesis of an AQ-dU nucleoside **1** with conjugation between the anthraquinone and the uridine moiety that could be employed in studies of charge-transfer processes in DNA (Fig. 1).[7] Here we disclose the synthesis of an AQ-dU nucleoside, its incorporation into oligonucleotides, and electrochemical studies of their use for detection of complementary oligonucleotides.

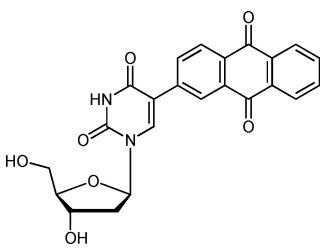

Fig. 1 AQ-dU nucleoside **1**.

For the construction of the C–C bond between the nucleobase and the anthraquinone moiety we aimed for the use of a Suzuki coupling employing an appropriate boronic ester derivative of anthraquinone and 2′-deoxy-5-iodouridine. As outlined in Scheme 1 two different boronic ester derivatives of anthraquinone were investigated. Starting from commercially available 2-bromoanthraquinone **2** the modified Miyaura procedure[8]

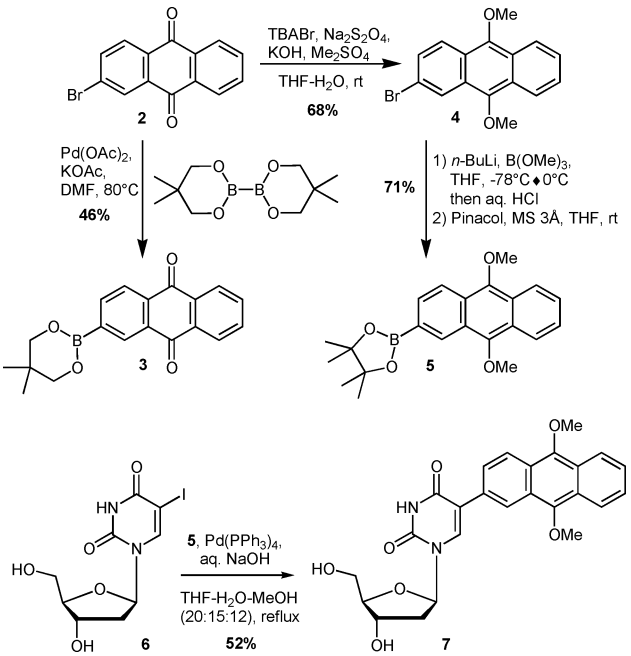

Scheme 1 Synthesis of AQ-dU nucleoside **1**.

furnished the anthraquinone boronic ester **3** in reasonable yield. The synthesis of the analogous pinacol ester of **3** by the Miyaura procedure[8] was unsuccessful.

Unfortunately, the subsequent Suzuki coupling with 2′-deoxy-5-iodouridine derivatives was unsuccessful, and led to extensive decomposition. Instead, the synthesis of dimethylated hydroquinone boronic ester **5** was carried out, that subsequent to any Suzuki reaction requires both demethylation and oxidation in order to reveal the anthraquinone motif. Hence, one-pot reduction and dimethylation of **2** yielded **4**. The organolithium species of **4** was subjected to borate trapping and further converted to the pinacolate **5** in good yield. Nucleoside **6** is rather insoluble in organic solvents, but it reacted well with **5** using a THF–MeOH–H_2O solvent mixture to afford **7** in 52% yield.

An efficient oxidative demethylation of **7** employing hypervalent iodine reagent PIFA[9] smoothly afforded pure **1** in 98% yield, which could be isolated by simple filtration (Scheme 2). The structure of **1** was confirmed by spectroscopic measurements, including

Danish National Research Foundation: Centre for DNA Nanotechnology (CDNA) at the Interdisciplinary Nanoscience Center (iNANO) and the Department of Chemistry, University of Aarhus, Langelandsgade 140, 8000 Aarhus C, Denmark. E-mail: kvg@chem.au.dk; Fax: +45 86196199

† Electronic supplementary information (ESI) available: Experimental procedures and spectroscopic data for compounds **1**, **4**, **5**, **7**, **8** and **9**, cyclic voltammogram of AQ-dU (**1**) and differential pulse voltammogram of O1 and O1+O3 duplex. See DOI: 10.1039/b816820b

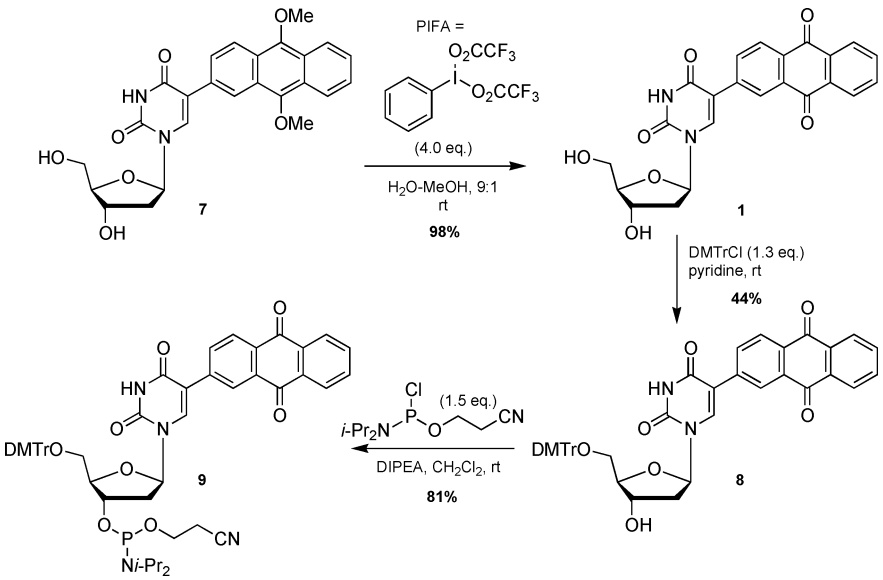

Scheme 2 Synthesis of phosphoramidite **10** for oligonucleotide synthesis.

ESI-mass spectrometry and 2D-NMR experiments, while NOE experiments confirmed the presence of a preferred *anti* glycosidic torsion angle in solution. The UV-Vis spectrum of a yellow EtOH-solution of **1** indicates a strong electronic interaction between the uridine moiety and the covalently attached anthraquinone as evident from the bathochromic shift of absorbance between **1** and pure anthraquinone (*e.g.* λ_{max} (anthraquinone) = 324 nm → λ_{max} (**1**) = 365 nm) (Fig. 2). Subsequently, protection of the 5′-hydroxyl group with DMTrCl gave **8** which could easily be converted into the phosphoramidites **9** required for oligonucleotide synthesis.

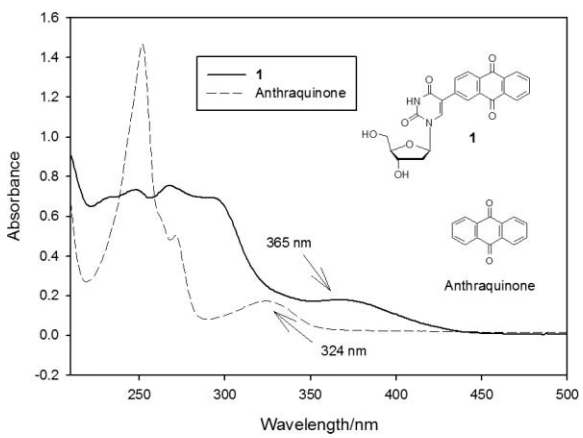

Fig. 2 UV-Vis spectrum of **1** and anthraquinone (both 50 μM in EtOH).

The incorporation of **9** into the oligonucleotide sequences **O1**[10], **O2** and **O6**[10] was carried out by standard automated solid-phase synthesis for phosphoramidite nucleosides on a DNA-synthesizer, which gave high coupling yields for **9**. Following standard deblocking and deprotection with aq. NH_3-solution, the oligonucleotide was purified by semi-preparative RP-HPLC and quantified by UV-Vis absorption spectroscopy. The identity of **O1**, **O2** and **O6** was confirmed by MALDI-TOF mass spectrometry (see ESI†).

Thermal denaturation experiments were performed in PBS-solution (Fig. 3 and Table 1). These duplexes exhibit cooperative, monophasic melting transitions. No hysteresis was observed for sequential heating–cooling cycles which demonstrate rapid hybridization kinetics.

O1: 5′-**Y**-CGA TCG A**X**C GAC TAG

O2: 5′-CGA TCG A**X**C GAC TAG

O3: 5′-CTA GTC GAT CGA TCG

O4: 5′-CGA TCG ATC GAC TAG

O5: 5′-CTA GTC GCT CGA TCG

O6: 5′-**Y**-TGG TCC TGT TCG CTC AAT CGT **X**CG GCT CGC

O7: 5′- GCG AGC CGA ACG ATT GAG CGA ACA GGA CCA

X = AQ-dU
Y = 5′-C6-disulphide modification:

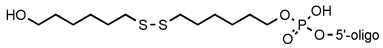

Fig. 3 Oligonucleotides for thermal denaturation and electrochemical studies.

Table 1 Thermal denaturation of duplexes[a]

Entry	Duplex	T_m/°C[b,c]
1	**O1/O3**	52.7
2	**O2/O3**	52.3
3	**O3/O4**	60.7
4	**O2/O5**	53.0
5	**O4/O5**	47.7

[a] Thermal denaturation was performed in PBS solution (1 M NaCl, 10 mM phosphate buffer, pH 7.0) on a Cary 100 UV-Vis spectrophotometer (Varian Inc.), and monitored at 260 nm with 1.0 °C min^{-1} in the range 15–90 °C using three cycles. 2 μM strand conc. [b] All T_m values are reproducible within ±1°C. [c] Melting temperatures were determined as the average of three heating–cooling cycles (six measurements).

The presence of 5′-disulfide modification in **O1** has virtually no influence on duplex stability compared to oligonucleotide **O2** (entries 1 and 2, Table 1). Evidently, the inclusion of AQ-dU into the oligonucleotide decreases the duplex stability compared to the unmodified duplex (entries 2 and 3). Furthermore, there is an absence of discrimination between matched and mismatched nucleotides for AQ-dU (entries 2 and 4), although AQ-dU stabilizes the duplex compared to a CT mismatch (entries 2 and 5). The melting transition of duplex **O1**/**O3** observed in the region 330–380 nm, where only AQ-dU absorbs, also shows significant hypochromicity which demonstrates the hydrophobic interactions of AQ-dU with adjacent bases (Fig. 4). Interestingly, these findings suggest that AQ-dU is mainly stabilizing the duplex by an intercalation mode of binding despite its hydrogen-bonding capacity.[11]

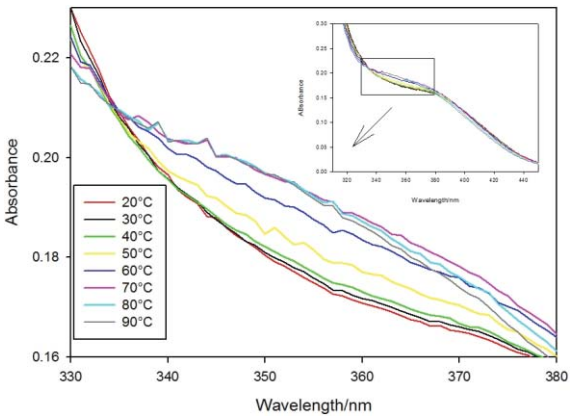

Fig. 4 Melting transition of AQ-dU in **O1**/**O3** duplex (10 mM phosphate buffer, 1.0 M NaCl, pH 7.0; 20 μM strand conc.).

We explored principal applicability of AQ-dU for electrochemical DNA assays. Cyclic voltammetry (CV) of an **O1**-modified gold electrode revealed a pair of redox peaks with a mean potential of –414 ± 3 mV (Fig. 5). These values are in a good agreement with the potential data obtained from the solution electrochemistry of AQ-dU, –422 ± 3 mV (see ESI†), which suggests that electrochemical features of the built-in DNA AQ-dU are close to those of the free AQ-dU base. The peak currents linearly depended on the potential scan rate, which is characteristic of surface-confined

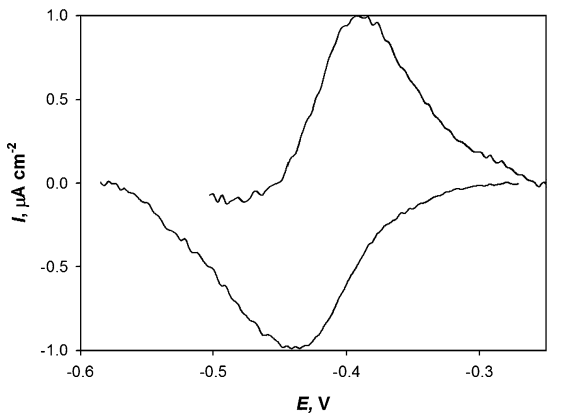

Fig. 5 Background-corrected cyclic voltammogram of a gold electrode modified with **O1**. Potential scan rate is 50 mV s^{-1}.

redox chemistry,[12] and the amount of the immobilized AQ-DNA, estimated from the redox peak area, was 8.4 ± 1.6 pmol cm^{-2} (data are averaged for 5 individual electrodes). This surface coverage corresponds to a loosely packed surface monolayer,[13] which is advantageous for surface hybridization assays. The electron transfer (ET) constant k_s, determined from the cathodic and anodic peak separation,[14] was 1.1 ± 0.2 s^{-1}. Considering negligible conductivity of a single-stranded (ss) DNA,[15] we assume that the observed ET phenomenon is due to the direct, *i.e.* non-mediated by DNA, ET reaction between the electrode and AQ moiety.

Upon hybridization of **O1** with a complementary strand **O3**, the AQ redox peak separation increased slightly, signifying that the kinetics of ET between AQ-dU and the electrode have not essentially changed. The k_s decreased to 0.8 ± 0.2 s^{-1}, and the redox potential for AQ-dU shifted only slightly to the less negative –411 ± 2 mV. These very minor variations in the ET kinetics may be ascribed to structural rearrangement of DNA due to hybridization, enabling, (a) directional ET through the dsDNA strands and, (b) less favorable "back-side" redox chemistry of AQ-dU. The persistence length of double-stranded (ds) DNA is around 50 nm, while that of ssDNA is around 1 nm.[16] Thus, with more flexible ssDNA, the redox probe can approach the electrode surface closer than with a more rigid dsDNA structure, where AQ-dU, fixed at a sequence predetermined position, should actually be removed from the electrode surface when **O1** hybridizes with **O3**. The presence of a one-point mutation (hybridization of **O1** with **O5**) did not produce any additional effects on the ET efficiency, which could be expected from thermal denaturation data. The matched **O1**–**O3** duplex has melting point characteristics close to those of the one-mismatch **O1(O2)**–**O5** duplex (Table 1).

In DNA assaying, one aims for clear discrimination between ssDNA and dsDNA states. As seen from the data above, it is difficult to achieve when AQ-dU is placed too close to the electrode surface. Therefore we extended this to investigate the electrochemistry of a 30 nts long AQ-dU DNA **O6**, which had AQ-dU modification in its 21 nt position relative the electrode surface (Fig. 3). For such ET distances, any ET in dsDNA is expected to be low, while non-directional ET reactions of a more flexible ssDNA are expected to proceed.

The CV of **O6** showed well-resolved AQ redox chemistry, though efficiency of ET was lower than that for **O1**: separation between AQ peaks corresponded to $k_s < 0.1$ s^{-1}. At scan rates higher than 20 mV s^{-1}, the cathodic peak shifted to the potentials of thiol desorption; thus for estimations of hybridization–dehybridization phenomena, we used the anodic peak clearly detectable in CVs (Fig. 6, inset). Upon hybridization of **O6** with complementary **O7**, the peak totally disappeared (Fig. 6), which is consistent with the removal of AQ-dU from the electrode surface upon the formation of a more rigid dsDNA structure. Hence, the efficiency of ET through the dsDNA appeared also to be very low at this distance. After subsequent dehybridization, the AQ oxidation peak reversibly appeared in the CV, and further disappeared upon the next hybridization process. This on–off redox process enabled us to electrochemically distinguish between ss and ds DNA surface states. It is worth mentioning that addition of a non-complementary DNA strand did not produce any changes in electrochemistry of **O6**.

In summary, we have devised an efficient synthesis of an AQ-derivatized nucleoside which is easily incorporated into

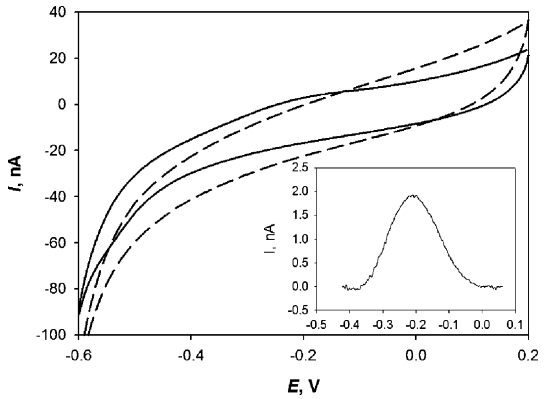

Fig. 6 Cyclic voltammetry for a gold electrode modified with **O6**, before (solid line) and after hybridization with a complementary **O7** (dashed line). Scan rate is 20 mV s^{-1}. Inset: background-subtracted peak for oxidation of AQ-dU, derived from the CV of **O6** in the main figure.

oligonucleotides. Electrochemical studies demonstrated principal applicability of the synthesized AQ-dU base for DNA assays. Future work will focus on the implementation of such oligonucleotides as photoexcitable probes for studies of DNA hole transport and the further development of the electrochemical DNA assays exploiting electrochemical and photochemical properties of the designed artificial nucleotide, *i.e.* estimations of effects of sequence positions of AQ-dU on selectivity and sensitivity of the DNA assay.

Acknowledgements

Financial support for this work by the Danish National Research Foundation, and the Carlsberg Foundation is gratefully acknowledged.

Notes and references

1 (*a*) H. Ihmels and D. Otto, *Top. Curr. Chem.*, 2005, **258**, 161–204; (*b*) D. Ly, Y. Kan, B. Armitage and G. B. Schuster, *J. Am. Chem. Soc.*, 1996, **118**, 8747–8748; (*c*) S. Kumamoto, M. Watanabe, N. Kawakami, M. Nakamura and K. Yamana, *Bioconjugate Chem.*, 2008, **19**, 65–69; (*d*) M. Castano-Alvarez, M. T. Fernandez-Abedul and A. Costa-Garcia, *Electrophoresis*, 2007, **28**, 4679–4689; (*e*) T. T. Williams, C. Dohno, E. D. A. Stemp and J. K. Barton, *J. Am. Chem. Soc.*, 2004, **126**, 8148–8158; (*f*) R. E. McKnight, J. Zhang and D. W. Dixon, *Bioorg. Med. Chem. Lett.*, 2004, **14**, 401–404; (*g*) S. Kumamoto, H. Nakano, Y. Matsuo, Y. Sugie and K. Yamana, *Electrochemistry*, 2002, **70**, 789–794.

2 (*a*) A. Okamoto, T. Kamei and I. Saito, *J. Am. Chem. Soc.*, 2006, **128**, 658–662; (*b*) A. Okamoto, T. Kamei, K. Tanaka and I. Saito, *J. Am. Chem. Soc.*, 2004, **126**, 14732–14733.

3 Review: H.-A. Wagenknecht, *Nat. Prod. Rep.*, 2006, **23**, 973–1006 and references therein.

4 *Charge-transfer in DNA: From mechanism to Application*, ed. H.-A. Wagenknecht, Wiley-VCH, Weinheim, 2005.

5 E. Mayer-Enthart and H.-A. Wagenknecht, *Angew. Chem., Int. Ed.*, 2006, **45**, 3372–3375.

6 C. Wagner and H.-A. Wagenknecht, *Chem.–Eur. J.*, 2005, **11**, 1871–1876.

7 A. A. Gorodetsky, O. Green, E. Yavin and J. K. Barton, *Bioconjugate Chem.*, 2007, **18**, 1434–1441.

8 L. Zhu, J. Duquette and M. Zhang, *J. Org. Chem.*, 2003, **68**, 3729–3732.

9 H. Tohma, H. Moriaka, Y. Harayama, M. Hashizume and Y. Kita, *Tetrahedron Lett.*, 2001, **42**, 6899–6902.

10 The 5′-C6-disulfide modification was incorporated such that the oligonucleotide may be immobilized on gold surfaces subsequently by standard thiol-Au chemistry.

11 (*a*) K. Yamana, Y. Nishijima, T. Ikeda, T. Gokota, H. Ozaki, H. Nakano, O. Sangen and T. Shimidzu, *Bioconjugate Chem.*, 1990, **1**, 319–324; (*b*) H. Deshmukh, S. P. Joglekar and A. D. Broom, *Bioconjugate Chem.*, 1995, **6**, 578–586.

12 A. J. Bard, and L. R. Faulkner, *Electrochemical Methods - Fundamentals and Applications*, Wiley, New York, 1980.

13 (*a*) M. Chahma, J. S. Lee and H. B. Kraatz, *J. Electroanal. Chem.*, 2004, **567**, 283–287; (*b*) K. A. Peterlinz and R. M. Georgiadis, *J. Am. Chem. Soc.*, 1997, **119**, 3401–3402; (*c*) D. Y. Petrovykh, H. Kimura-Suda, L. J. Whitman and M. J. Tarlov, *J. Am. Chem. Soc.*, 2003, **125**, 5219–5226; (*d*) A.-E. Radi, J. L. A. Sánchez, E. Baldrich and C. K. O'Sullivan, *J. Am. Chem. Soc.*, 2006, **128**, 117–124.

14 E. Laviron, *J. Electroanal. Chem.*, 1979, **101**, 19–28.

15 G. Hartwich, D. J. Caruana, T. de Lumley-Woodyear, Y. Wu, C. N. Campbell and A. Heller, *J. Am. Chem. Soc.*, 1999, **121**, 10803–10812.

16 S. B. Smith, Y. Cui and C. Bustamante, *Science*, 1996, **271**, 795–799.

